JOURNAL OF MATERIALS SCIENCE 28 (1993) 4623–4629

Comparison of strengthening in wire-drawn or rolled Cu–20% Nb with a dislocation accumulation model

W. A. SPITZIG, S. B. BINER
Ames Laboratory USDOE, Iowa State University, Ames, IA 50011, USA

Strengthening after large deformations by wire-drawing or rolling of Cu, Nb and Cu–20% Nb was compared with the predictions of a proposed modified substructural strengthening model for ductile two-phase alloys. The comparisons indicate that the more extensive and refined model of Funkenbusch and Courtney offers no improvement over the original model of Ashby in predicting the strengthening with increased deformation processing or the dislocation densities necessary to produce the observed strengthening in Cu–20% Nb. Both models can predict the strengthening behaviour of Cu–20% Nb. However, neither model is in accord with the observations that the dislocation density in the Cu matrix is essentially independent of the degree of deformation processing, and that the magnitudes of the dislocation density are much the same in the Cu in Cu–20% Nb and pure Cu identically deformation-processed. In addition, there is no experimental support for the Funkenbusch and Courtney model prediction of an order of magnitude greater dislocation density in the Nb filaments than in the Cu matrix in Cu–20% Nb. It appears that a mechanism that does not require an accumulation of dislocations for strengthening, such as the difficulty in propagating dislocations between closely spaced barriers, is more likely to be responsible for strengthening in Cu–Nb-type deformation-processed composites.

1. Introduction

In a recent exchange of comments [1, 2] on the relative merits of interphase barrier or dislocation accumulation models for predicting strengthening in deformation-processed Cu–20% Nb, results were presented for the predicted dislocation densities in the Cu matrix based on a modified non-homogeneous deformation model [3, 4]. According to these results the predicted dislocation densities in the Cu matrix appeared to be in reasonable agreement with the experimental measurements. This seemed to give credence to the proposal that dislocation accumulation as a result of non-homogeneous deformation, because of incompatibility between Cu and Nb, was the primary cause of strengthening in Cu–20% Nb [5–7]. However, recent work [8] has shown that this also gives credence to a barrier model where the Cu–Nb interfaces are assumed to act as sources of dislocations which control plastic flow across the interfaces [9, 10] because this model gave similar predictions of dislocation accumulation during deformation processing as a non-homogeneous deformation model [11]. Although in this recent work [8] the dislocation densities predicted by both the barrier and non-homogeneous model were similar, their magnitudes were significantly larger than the measured values or those values indicated as predicted by the modified non-homogeneous deformation model [3, 4], and both models were deemed inadequate for explaining strengthening in Cu–20% Nb. To gain better insight into the modified non-homogeneous model [5, 6], results obtained for wire-drawn or rolled Cu, Nb and Cu–20% Nb were used to explore the substructural predictions of the model in greater detail than presented previously [3, 4]: in particular, the predictions of the dislocation densities in both the Cu and Nb in Cu–20% Nb after various degrees of deformation processing. The dislocation densities in the Nb in Cu–20% Nb are of significant interest because it has been proposed that it is this phase that primarily controls the strengthening behaviour in alloy systems such as Cu–Fe and Cu–Nb where the Cu phase undergoes saturation hardening during deformation processing [5, 7]. No mention was made of the predicted dislocation densities in the Nb phase in the previous analysis [3, 4].

2. Experimental procedure

Two ingots of Cu containing 20 vol % Nb were prepared by consumable arc-melting electrodes containing Nb strips in a Cu cylinder as previously described [12]. One ingot was about 6.35 cm in diameter and about 20 cm in length. The diameter of this ingot was machined down to about 6.1 cm and the ingot was rod-rolled to 1.3 cm in a series of steps and subsequently drawn into wires at room temperature using successively smaller dies to a minimum diameter of 0.15 mm. The second ingot was about 7.6 cm in diameter and about 20 cm in length. The diameter of this ingot was machined to 7.4 cm and diametrically opposite flats were machined on the ingot to give a nearly

0022–2461

rectangular cross-section of 6.1 cm by 7.4 cm. This ingot was rolled at room temperature from 6.1 cm to a minimum thickness of 0.064 mm. A 6.1 cm diameter rod of the Cu and a 6.1 cm casting of the Nb used in the electrodes were processed in the same manner as the Cu–20% Nb alloys.

Tensile specimens with a 2.8 cm gauge length were machined from wires drawn down to 0.25 cm, while the smaller-diameter wires were used directly by embedding their ends into Cu sleeves which were used as grip ends. Tensile specimens were machined from the rolled sheet at various thicknesses down to 0.064 mm. Their gauge cross-section was 0.5 cm by the sheet thickness and the gauge length was 2.8 cm. All tensile tests were done at room temperature using an initial strain rate of $1.7 \times 10^{-4}\ s^{-1}$. At least three specimens were tested at each wire and sheet size and reproducibility was within 3%. The mechanical properties and microstructural development have been previously reported for the wire-drawn [13] and rolled [14] Cu–20% Nb. The mechanical properties of Cu and Nb after deformation processing by wire drawing [15, 16] and of Cu after deformation processing by rolling [8] have been reported earlier. The mechanical properties of rolled Nb, like those of rolled Cu [8], were similar to those obtained for wire-drawn Nb when compared on the basis of effective strains [17].

3. Dislocation-strengthening model

The results for strengthening in wire-drawn and rolled Cu–20% Nb will be analysed using a previously proposed model for strengthening in deformation-processed two-phase alloys [5, 6], which is based on a modified rule-of-mixtures criterion

$$\sigma_c = V_{Cu}\sigma_{Cu} + V_{Nb}\sigma_{Nb} \quad (1)$$

where V is the volume fraction and σ is the flow stress of each metal. The flow stresses of Cu and Nb are assumed to be given by

$$\sigma = \sigma_0 + \alpha M G b \rho^{1/2} \quad (2)$$

where σ and σ_0 are tensile stresses, G is the shear modulus, b is the Burgers vector and α and M are constants. The dislocation densities in the Cu and Nb phases are assumed to vary with deformation strain, η, and interphase spacing, λ, according to

$$\frac{d\rho}{d\eta} = C_1\rho^{1/2} - C_2\rho + \frac{PK}{V\lambda} \quad (3)$$

where C_1 and C_2 are constants for each phase, P is a dislocation partition coefficient having potential values between 0 and 1 and K is a constant accounting for plastic incompatibility between Cu and Nb [5, 6].

This model is a modification of the Ashby model of non-homogeneous deformation in two-phase alloys [11] for adaptation to the large-strain behaviour observed in ductile two-phase alloys. In the Ashby model [11] the dislocation densities derive essentially from the third term in Equation 3. In this model the geometrical dislocation density, ρ_G, can be expressed as [8]

$$\rho_G = \frac{4K_1 \tan^{-1}\gamma}{b\lambda} \quad (4)$$

where b is the Burgers vector, γ is the shear strain and K_1 is a compatibility constant but different in magnitude to K in Equation 3. In the Ashby model ρ_G is substituted for ρ in Equation 2 to calculate the tensile strength of the two-phase material. Therefore the Funkenbusch and Courtney model [5, 6] uses the total dislocation density, statistical and geometrical dislocations, while the Ashby model [11] uses only the geometrically necessary dislocations. In two-phase alloys the statistical dislocations predominate at small strains while the geometrical dislocations predominate at large strains.

Values of M, the Taylor factor, in Equation 2 depend on the texture of the polycrystalline metal. The generally accepted initial value for undeformed Cu is about 3.1 [18, 19] and it increases with increasing deformation to an expected value of about 3.4 during subsequent deformation processing [19]. In b.c.c. metals M is expected to have a value near 2.8 initially [19] but the $\langle 1\,1\,0 \rangle$ texture that develops causes the metal to deform under plane strain rather than axisymmetric flow and the value of M is expected to be about 2.1 after subsequent deformation processing [20]. Using the value $\alpha = 0.3$ measured in Cu single crystals [21] and taking $M = 3.1$ results in $\alpha M = 0.93$ for Cu, which is very similar to the values of $\alpha M = 1.0$–1.14 measured in polycrystalline Cu [22, 23]. In polycrystalline Nb, $\alpha M = 0.85$ [24]. Therefore, $\alpha M \simeq 1$ for both Cu and Nb in Equation 1. Further support for $\alpha M \simeq 1$ in both f.c.c. and b.c.c. metals is shown by more extensive dislocation density determinations in Al and Fe [19]. In Al, αM ranges from 0.70 to 1.25 and in Fe, αM ranges from 0.76 to 1.4. Therefore, we have taken $\alpha M = 1.14$ in Cu, the average of the measured values (1.03) for single-crystal and polycrystalline Cu [21–23] increased by 10% to take into account the predicted increase in M with subsequent deformation processing [19]. For Nb we have used $\alpha M = 1$, even though M is expected to decrease with increasing deformation processing [20]. Based on the results in the literature, these values of αM seem to be reasonable for Cu and Nb. The same values were used for wire-drawn or rolled Cu–20% Nb.

These values for αM contrast with the previous arbitrary assumption that $\alpha M = 3$ for both Cu and Nb [5, 6]. Although the value of αM does not affect the trends obtained from the analysis, using $\alpha M = 3$ instead of ~ 1 in Equation 2 results in about an order of magnitude decrease in the predicted dislocation densities for a given strength level. While the original formulation of the model did not determine the predicted dislocation densities in the Cu and Nb phases [5, 6], although subsequent work showed the predicted dislocation densities in the Cu phase assuming $\alpha M = 3$ [3, 4], direct comparison of the observed strengths and dislocation densities in the Cu–20 % Nb studied here makes the values used for αM for the Cu and Nb phases important.

For Cu–20% Nb, P is taken as 0.5 for both Cu and Nb because both phases appear to deform equally [5, 6] and λ is given by

$$\lambda/\lambda_0 = \exp(-0.36\eta) \quad (5)$$

for wire-drawn material [13] and by

$$\lambda/\lambda_0 = \exp(-0.74\eta) \quad (6)$$

for rolled material [14]. In Equation 5, $\eta = 2\ln(d_0/d)$ where d_0 and d are the initial and final wire diameters, respectively. In Equation 6, $\eta = \ln(h_0/h)$ where h_0 and h are the initial and final sheet thicknesses. Equations 5 and 6 also apply for the reduction in Nb filament size (t) with deformation processing. The initial sizes of λ and t are designated λ_0 and t_0, which are 24.8 and 6.2 μm, respectively, for wire-drawn [13] and 25.6 and 6.4 μm for rolled [14] Cu–20% Nb. Values used for G and b in Equation 2 were 48.3 GPa and 0.26 nm, respectively, for Cu and 37.5 GPa and 0.29 nm for Nb.

Figs 1 and 2 show the tensile stress data for pure Cu and Nb, respectively, wire-drawn to reductions up to $\eta = 11.9$. On these figures are plotted the predicted curves for pure Cu and Nb. While the models consider the flow stresses, the ultimate tensile stress was used for comparison purposes because it was very reproducible and well defined. In addition, because of the pronounced work-hardening in the deformation-processed specimens during initial straining an offset stress criterion for the flow stress was inaccurate. Because the uniform elongations were small ($\leq 2\%$) in the deformation-processed wires and sheets, the ultimate tensile stress should be a good representation of the flow stress for comparison with the models. Values for the constants C_1 and C_2 along with the values used for σ_0 for Cu and Nb are shown in Figs 1 and 2. The values for C_1 and C_2 were obtained by fitting the experimental strength data shown in Figs 1 and 2 for pure Cu and Nb, deformation-processed in a similar manner to Cu–20% Nb, to Equation 3 with the term $PK/V\lambda$ set to zero. Values used for σ_0 corresponded to the yield strengths of the initial pure Cu and Nb. The fit of the predicted curves to the experimental results appears reasonable in view of the use of numerical integration techniques to obtain the values for C_1 and C_2.

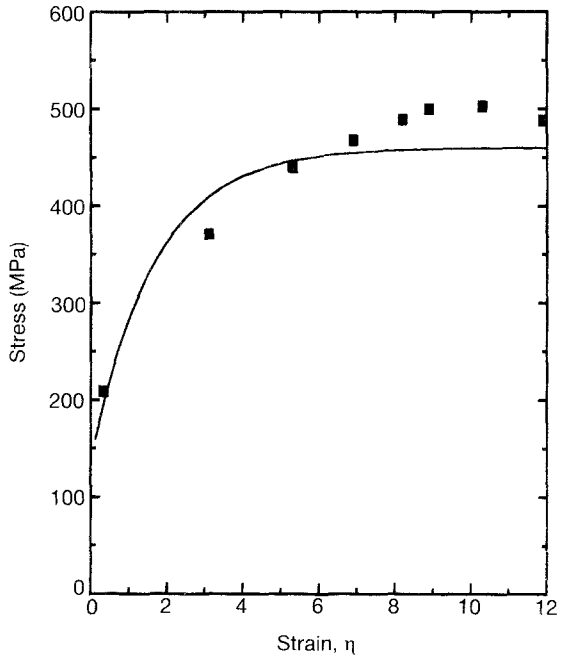

Figure 1 Comparison of (——) predicted and (■) observed effect of deformation processing by wire-drawing on the tensile stress of Cu. Constants used to construct the predicted curve are $\sigma_0 = 45$ MPa, $\alpha M = 1.14$, $C_1 = 3.48 \times 10^7\ m^{-1}$, $C_2 = 1.2$.

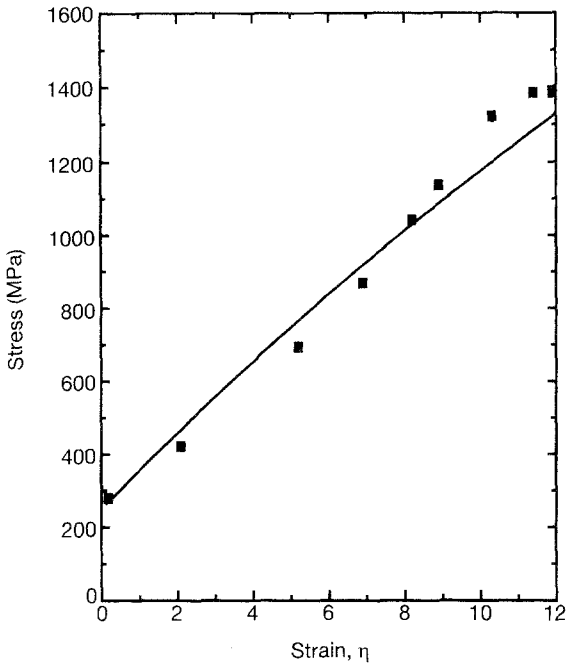

Figure 2 Comparison of (——) predicted and (■) observed effect of deformation processing by wire drawing on the tensile stress of Nb. Constants used to construct the predicted curve are $\sigma_0 = 200$ MPa, $\alpha M = 1.0$, $C_1 = 2.0 \times 10^7\ m^{-1}$, $C_2 = 0.06$.

Using these fitted values for C_1 and C_2 for Cu and Nb in Equation 3, Equation 5 for λ, taking $P = 0.5$, $V = 0.8$ and 0.2 for Cu and Nb, respectively, results in a value for K that produces agreement with the experimental observations of strength with increasing deformation processing. The model predictions are shown in Fig. 3 for $K = 5.0 \times 10^9\ m^{-1}$, which gives good agreement with the experimental observations at the larger strain values. As observed previously in the application of this model to various two-phase alloy systems [6], a constant K value does not give a good fit throughout the deformation processing range ($\eta = 3.1$–11.9). Using this value for K in Equation 3 results in the predicted dislocation densities shown in Fig. 4 for the Cu and Nb phases in Cu–20% Nb. Included in Fig. 4 are measured dislocation densities at $\eta = 11$ for pure Cu and for Cu in Cu–20% Nb using high-voltage TEM [25]. These values are the maximum dislocation densities measured and not average values. Numerous regions occurred that were devoid of dislocations and these were not taken into consideration in determining the dislocation densities reported [25]. Also included at small strains are dislocation densities measured on polycrystalline Cu [22, 23] and a curve for $K = 0$, representing the predicted dislocation densities in pure Cu. The curve for $K = 0$ is in reasonable agreement with the measured dislocation densities in pure Cu at both small and

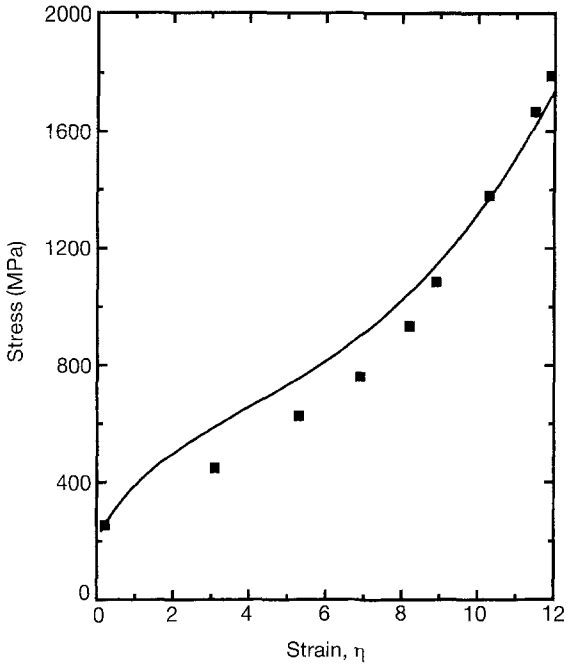

Figure 3 Comparison of (——) predicted and (■) observed effect of deformation processing by wire drawing on the tensile stress of Cu–20% Nb. The K parameter used to construct the predicted curve is 5.0×10^9 m^{-1}. Values of the other constants are the same as in Figs 1 and 2.

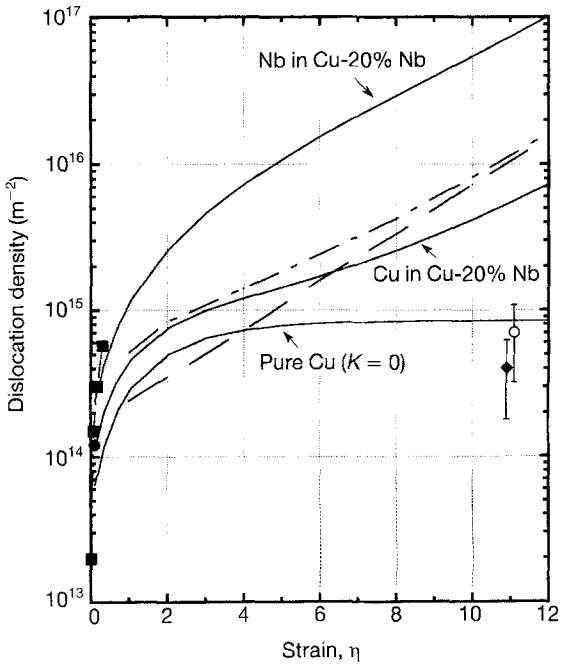

Figure 4 (——) Predicted dislocation densities in the Cu and Nb in Cu–20% Nb after deformation processing by wire-drawing, together with predictions by (— —) the Ashby model and (— · —) the Ashby model added to the $K = 0$ curve. Included are measured dislocation densities in (■, ●, ◆) Cu and (○) Cu in Cu–20% Nb. The K parameter used to construct the predicted curves is 5.0×10^9 m^{-1}. Values of the other constants are the same as in Figs 1 and 2.

large strains. Other results for pure Cu and Cu–20% Nb deformation-processed by wire-drawing using regular TEM measured dislocation densities between 10^{14} and 10^{15} m^{-2} for pure Cu and for Cu and Nb in Cu–20% Nb, independent of the degree of deformation strain [13, 26].

Also included in Fig. 4 are curves showing the predicted dislocation densities in the Cu in Cu–20% Nb using the Ashby model with no rule-of-mixtures criterion [8, 11]. The initial lower values of dislocation density predicted by the Ashby model [11] result from the model predicting only the geometrical dislocation density, whereas, the Funkenbusch and Courtney model [5, 6] predicts the total dislocation density. At large strains the geometrical dislocation density is expected to predominate in accord with the observed similar predictions of dislocation density by both models. At smaller strains the statistical dislocations are expected to predominate, i.e. the first two terms in Equation 3. The effect of adding the statistical dislocation densities predicted by the $K = 0$ curve in Fig. 4 to the geometrical dislocation densities predicted by the Ashby model [11] is also shown in Fig. 4. This curve for the total dislocation density predicted using the Ashby model is similar to that shown for the total dislocation density in Cu by the Funkenbusch and Courtney model [5, 6]. Comparison of the predicted dislocation densities in Cu in Cu–20% Nb from either model with the previous TEM measurements shows poor agreement. Particularly in contrast to the predictions of the models are the TEM observations indicating that there is little if any difference in the dislocation densities in identically deformation-processed pure Cu and the Cu in Cu–20% Nb. In addition, the few measurements that have been made of the dislocation densities in the Nb filaments show densities equivalent to those measured in the Cu matrix [13, 24], not an order of magnitude greater as indicated in Fig. 4. Therefore, both the Ashby [8, 11] and the Funkenbusch and Courtney [5, 6] models show a poor correlation with the measured dislocation densities shown at $\eta = 11$ in Fig. 4 and those measured previously [13, 26] at deformation strains between $\eta = 3.6$ and 11.9 ($10^{14} - 10^{15}$ m^{-2}).

Fig. 5 shows the predicted stresses in the Cu and Nb phases in Cu–20% Nb based on the predicted dislocation densities shown in Fig. 4 for each phase. Also included in Fig. 5 are the predicted and the experimentally measured stresses for Cu–20% Nb from Fig. 3. The Cu in Cu–20% Nb is predicted to develop increasing strength with increasing deformation processing, similar to Cu–20% Nb. The maximum stress attained in the Cu in Cu–20% Nb at $\eta = 11.9$ is about 2.5 times greater than the maximum stress measured in pure Cu at this strain (Fig. 1). Likewise, the maximum stress predicted in the Nb filaments in Cu–20% Nb at $\eta = 11.9$ is more than 2.5 times greater than that measured in pure Nb (Fig. 2). These predictions that the Cu and Nb phases in Cu–20% Nb can attain stresses of about 1260 and 3650 MPa, respectively, do not appear reasonable and have no experimental support. In addition, the prediction that the Cu in Cu–20% Nb exhibits exponential hardening is in sharp contrast to the observed saturation hardening that occurs in pure Cu (Fig. 1) and the similarity in dislocation structures observed in pure Cu and the Cu in Cu–20% Nb [13].

Similar calculations were carried out for Cu, Nb and Cu–20% Nb deformation-processed by rolling to

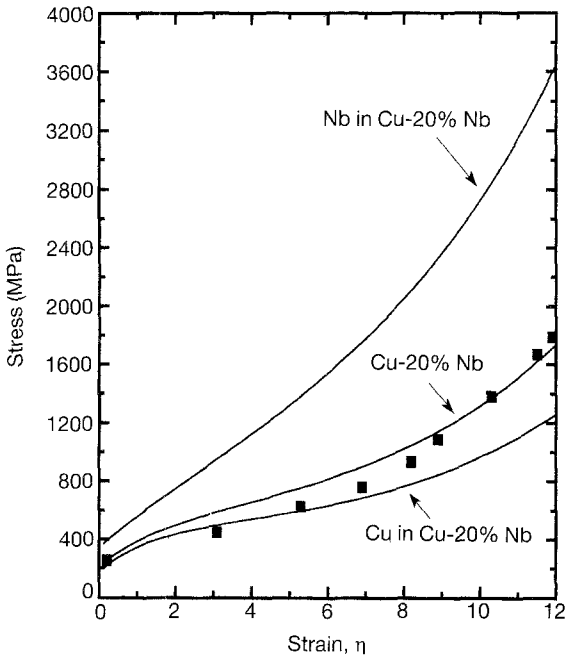

Figure 5 (——) Predicted tensile stresses in the Cu and Nb in Cu–20% Nb and in Cu–20% Nb after deformation processing by wire-drawing, together with (■) experimental data for Cu–20% Nb. The parameter K used to construct the predicted curves is $5.0 \times 10^9\ m^{-1}$. Values of the other constants are the same as (—) in Figs 1 and 2.

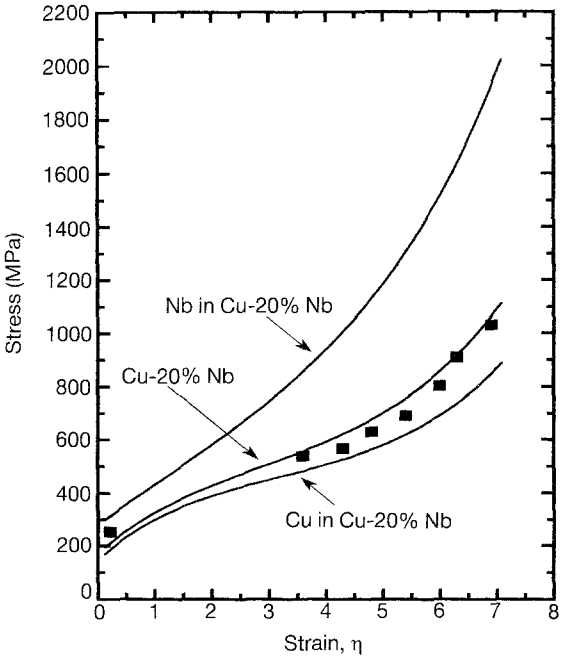

Figure 6 (——) Predicted tensile stresses in the Cu and Nb in Cu–20% Nb and in Cu–20% Nb after deformation processing by rolling, together with (■) experimental data for Cu–20% Nb. The parameter K used to construct the predicted curves is $1.0 \times 10^9\ m^{-1}$. Values of the other parameters are the same as in Figs 1 and 2.

$\eta = 6.9$. Figs 6 and 7 show the stress and dislocation density predictions, respectively, with processing strain. Values used for the constants C_1 and C_2 along with the values used for σ_0 for Cu and Nb were the same as those used for wire-drawn Cu and Nb (Figs 1 and 2). There was no significant difference in the tensile strength behaviour of rolled or wire-drawn material. Using these fitted values for C_1 and C_2 for Cu and Nb in Equation 3, Equation 6 for λ, taking $P = 0.5$, $V = 0.8$ and 0.2 for Cu and Nb, respectively, results in a value for K that is in agreement with the experimental observations of strength with increasing deformation processing. The model predictions are shown in Fig. 6 for $K = 1.0 \times 10^9\ m^{-1}$. The K value required for rolled Cu–20% Nb is smaller than the one necessary for wire-drawn Cu–20% Nb. This is similar to what is observed in using the Ashby model [8]. The fit of observed and predicted stresses is quite good using a K value of $1.0 \times 10^9\ m^{-1}$. Using this value for K in Equation 3 results in the predicted dislocation densities shown in Fig. 7 for the Cu and Nb phases in Cu–20% Nb. Included in Fig. 7 are measured dislocation densities using high-voltage TEM for pure Cu, for Cu in Cu–20% Nb and for Nb filaments extracted from Cu–20% Nb [27]. These densities were obtained from regions showing maximum dislocation densities, and are not average values. Also included in Fig. 7 is a curve for $K = 0$ representing the predicted dislocation densities in pure Cu. The curve for $K = 0$ is in good agreement with the measured dislocation densities in pure Cu. Comparison of the predicted dislocation densities in the Cu matrix in Cu–20% Nb with the previous TEM measurements shows poor agreement at the larger

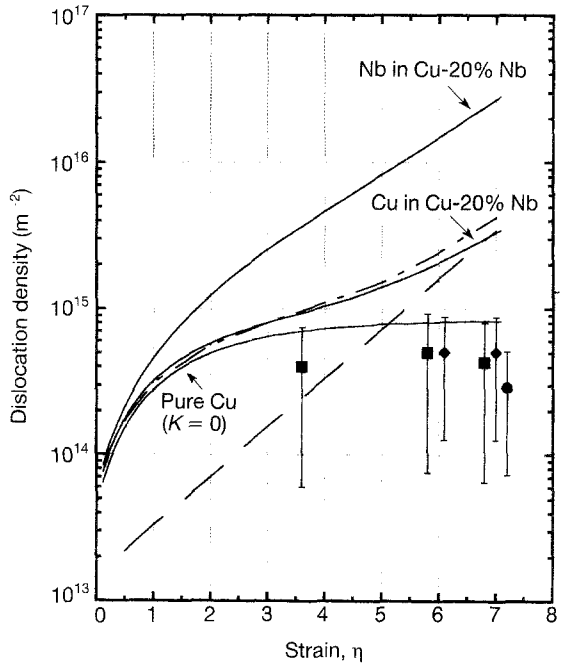

Figure 7 (——) Predicted dislocation densities in the Cu and Nb in Cu–20% Nb after deformation processing by rolling, together with predictions by (— —) the Ashby model and (— · —) the Ashby model added to the $K = 0$ curve. Included are measured dislocation densities in (●) Cu and in (■) Cu and (◆) Nb in Cu–20% Nb. The parameter K used to construct the predicted curves is $1.0 \times 10^9\ m^{-1}$. Values of the other constants are the same as in Figs 1 and 2.

strains. Also the observation that at $\eta = 6$ and 6.9 the dislocation density in the Nb filaments in Cu–20% Nb is similar to that in the Cu matrix [14] is in disagreement with the significantly greater predicted dislocation density in Nb. Also included in Fig. 7 are curves

of the predicted dislocation densities in the Cu in Cu–20% Nb using the Ashby model [8, 11]. The predicted values for the total dislocation densities are similar to those predicted from the Funkenbusch and Courtney model [5, 6] when the statistical dislocation densities (K = 0 curve in Fig. 7) are added to the geometrically necessary dislocations predicted by the Ashby model [8]. The predicted stresses in the Cu and the Nb in rolled Cu–20% Nb (Fig. 6) by the Funkenbusch and Courtney model [5, 6] are essentially the same as those shown for wire-drawn Cu–20% Nb in Fig. 5 when compared on the basis of effective strains.

The effect of taking $\alpha M = 3$ in Equation 2, as was previously done [5, 6], is shown in Figs 8 and 9 for wire-drawn Cu–20% Nb. Values for the constants C_1, C_2 and K are shown in Fig. 8. The fitted values obtained for C_1 and C_2 for the Cu used in this study are smaller and the value of K needed to get a reasonable fit with the stress data is larger than those used previously [5, 6]. Previous values used for C_1 and C_2 for Nb do not appear to have been reported [3–6]. The value of K needed to get a reasonable fit with the experimental results is decreased by an order of magnitude as a result of increasing αM from about 1 to 3 (compare Figs 3 and 8). Fig. 8 is almost identical to Fig. 5. The biggest effect of increasing the value of αM is in decreasing the predicted dislocation densities as shown by comparing Fig. 9 with Fig. 4. While the trend of the curves remains similar, the curves are displaced to significantly lower values of dislocation density as αM increases. As discussed earlier, experimental evidence for Cu [21–23] and Nb [24] supports $\alpha M \simeq 1$ as a realistic value. Also included in Fig. 9 are

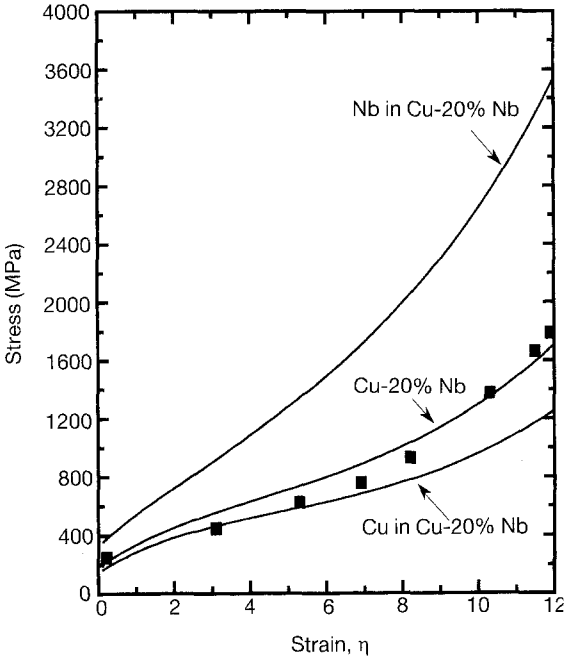

Figure 8 (——) Predicted tensile stresses in the Cu and Nb in Cu–20% Nb and in Cu–20% Nb after deformation processing by wire-drawing, together with (■) experimental data for Cu–20% Nb. Values of the constants used to construct the predicted curve are as follows: for Cu, $C_1 = 8.71 \times 10^6\ m^{-1}$ and $C_2 = 0.738$; for Nb, $C_1 = 6.45 \times 10^6\ m^{-1}$ and $C_2 = 0.049$; $K = 5.0 \times 10^8\ m^{-1}$. Values used for σ_0 were the same as in Figs 1 and 2, and $\alpha M = 3$ was used for both Cu and Nb.

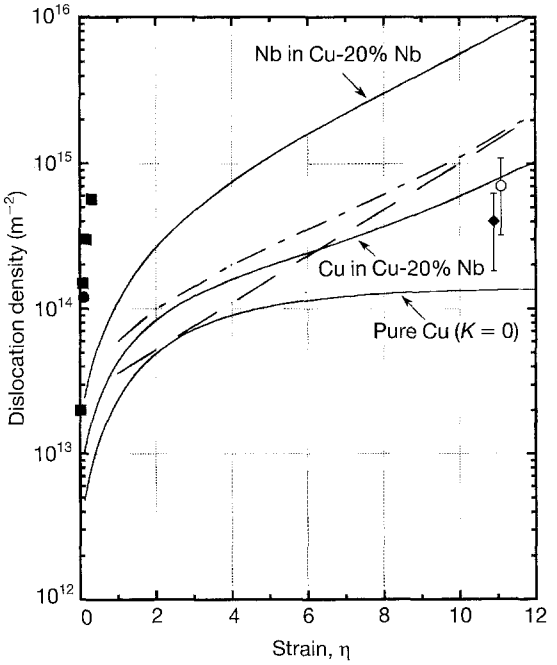

Figure 9 (——) Predicted dislocation densities in the Cu and Nb in Cu–20% Nb after deformation processing by wire-drawing, together with predictions by (— —) the Ashby model and (— · —) the Ashby model added to the $K = 0$ curve. Included are measured dislocation densities in (■, ●, ◆) Cu and in (○) Cu in Cu–20% Nb. The parameter K used to construct the predicted curves is $5.0 \times 10^8\ m^{-1}$. Values used for σ_0 were the same as in Figs 1 and 2, and $\alpha M = 3$ was used for both Cu and Nb.

curves of the predicted dislocation densities in the Cu in Cu–20% Nb using the Ashby model with $\alpha M = 3$ [8, 11]. Again, the predicted values for the total dislocation densities, when the statistical dislocation densities ($K = 0$ curve) are added to the geometrical dislocation densities predicted by the Ashby model [8, 11], are similar to those predicted for the Cu in Cu–20% Nb by the Funkenbusch and Courtney model [5, 6]. However, taking $\alpha M = 3$ results in predicted dislocation densities in pure Cu ($K = 0$ curve in Fig. 9) that are significantly lower than those measured at both small and large strains. This further supports the use of $\alpha M \simeq 1$ rather than 3 as being more realistic.

Recent work [8] has shown that a barrier model for strengthening in Cu–20% Nb also predicted dislocation densities equivalent to those predicted by the dislocation accumulation model of Ashby [11], indicating that barrier models as a probable explanation of strengthening in Cu–20% Nb suffer from the same shortcomings as the dislocation accumulation models. It appears that a mechanism that does not require accumulation of dislocations for strengthening is more likely to be responsible for strengthening in Cu–Nb-type deformation-processed composites. A model based on the difficulty in propagating dislocations between closely spaced barriers may offer a possible alternative mechanism. Recent preliminary work has shown that a dislocation propagation model [28] for strengthening in deformation-processed Cu–20% Nb wires was in good agreement with experimental results when more accurate measurements of filament spacings in the heavily deformed wires, obtained using

high-voltage conical-scan dark-field TEM, were used in the model [29].

4. Conclusion

It appears that the more extensive and refined model of Funkenbusch and Courtney [5, 6] offers no improvement over the original model of Ashby [8, 11] in predicting the strengthening with increased deformation processing of Cu–20% Nb and the dislocation densities necessary to produce the observed strengthening. However, neither model is in accord with the observations that the dislocation density in the Cu matrix is essentially independent of the degree of deformation processing or that the magnitudes of the dislocation density are much the same in the Cu in Cu–20% Nb and pure Cu identically deformation-processed. It appears that a model [28] based on the difficulty in propagating dislocations, rather than accumulating dislocations, between closely spaced barriers is more likely to be responsible for strengthening in Cu–Nb-type deformation-processed composites [29].

Acknowledgements

This work was performed for the US Department of Energy by Iowa State University under contract No. W-7405-Eng-82. This research was supported by the Director of Energy Research, Office of Basic Energy Sciences.

References

1. W. A. SPITZIG, J. D. VERHOEVEN, C. L. TRYBUS and L. S. CHUMBLEY, *Scripta Metall.* **24** 1171.
2. *Idem, ibid.* **24** (1990) 1181.
3. P. D. FUNKENBUSCH and T. H. COURTNEY, *ibid.* **24** (1990) 1175.
4. *Idem, ibid.* **24** (1990) 1183.
5. *Idem, Acta Metall.* **33** (1985) 913.
6. *Idem, Metall. Trans.* **18** (1987) 1249.
7. *Idem, Scripta Metall.* **23** (1989) 1719.
8. W. A. SPITZIG, *Acta Metall.* **39** (1991) 1085.
9. J. C. M. LI and Y. T. CHOU, *Metall. Trans.* **1** (1970) 1145.
10. J. C. M. LI, *Trans. AIME* **227** (1963) 239.
11. M. F. ASHBY, in "Strengthening Methods in Crystals", edited by A. Kelly and R. B. Nicholson (Wiley, New York, 1971) p. 137.
12. J. D. VERHOEVEN, F. A. SCHMIDT, E. D. GIBSON and W. A. SPITZIG, *J. Metals* **39** (9) (1986) 20.
13. W. A. SPITZIG, A. R. PELTON and F. C. LAABS, *Acta Metall.* **35** (1987) 2427.
14. C. L. TRYBUS and W. A. SPITZIG, *ibid.* **37** (1989) 1971.
15. W. A. SPITZIG and P. D. KROTZ, *Scripta Metall.* **21** (1987) 1143.
16. W. A. SPITZIG, Ames Laboratory, Iowa State University, unpublished research, (1991).
17. W. A. SPITZIG, C. L. TRYBUS and F. C. LAABS. *Mater. Sci. Engng.* **A145** (1991) 179.
18. I. LE MAY, "Principles of Mechanical Metallurgy" (Elsevier, New York, 1981) pp. 124 and 187.
19. J. GIL SEVILLANO, P. van HOUTTE and E. AERNOUDT, *Prog. Mater. Sci.* **25** (1981) 69.
20. W. F. HOSFORD Jr, *Trans. AIME* **230** (1964) 12.
21. J. D. LIVINGSTON, *Acta Metall.* **1** (1962) 229.
22. J. E. BAILEY, *Philos. Mag.* **8** (1963) 223.
23. M. R. STAKER and D. L. HOLT, *Acta Metall.* **20** (1972) 569.
24. L. I. Van TORNE and G. THOMAS, *ibid.* **1** (1963) 881.
25. L. S. CHUMBLEY, H. L. DOWNING, W. A. SPITZIG and J. D. VERHOEVEN, *Mater. Sci. Engng* **A117** (1989) 59.
26. A. R. PELTON, F. C. LAABS, W. A. SPITZIG and C. C. CHENG, *Ultramicrosc.* **22** (1987) 251.
27. C. L. TRYBUS, L. S. CHUMBLEY, W. A. SPITZIG and J. D. VERHOEVEN, *ibid.* **30** (1989) 315.
28. J. GIL SEVILLANO, in "Strength of Metals and Alloys", Proceedings of ICSMA 5, edited by P. Haasen, V. Gerold and G. Kostorz (Pergamon, Oxford, 1980) p. 819.
29. J. D. VERHOEVEN, L. S. CHUMBLEY, F. C. LAABS and W. A. SPITZIG, *Acta Metall.* **39** (1991) 2825.

Received 13 March 1992
and accepted 25 January 1993